Editors' Suggestion

Quantum Criticality of Antiferromagnetism and Superconductivity with Relativity

Hanqing Liu,[1] Emilie Huffman,[2] Shailesh Chandrasekharan,[1] and Ribhu K. Kaul[3]
[1]Department of Physics, Box 90305, Duke University, Durham, North Carolina 27708, USA
[2]Perimeter Institute for Theoretical Physics, Waterloo, Ontario N2L 2Y5, Canada
[3]Department of Physics and Astronomy, University of Kentucky, Lexington, Kentucky 40506, USA

(Received 21 September 2021; accepted 14 February 2022; published 15 March 2022)

We study a quantum phase transition from a massless to massive Dirac fermion phase in a new two-dimensional bipartite lattice model of electrons that is amenable to sign-free quantum Monte Carlo simulations. Importantly, interactions in our model are not only invariant under SU(2) symmetries of spin and charge like the Hubbard model, but they also preserve an Ising-like electron spin-charge flip symmetry. From unbiased fermion bag Monte Carlo simulations with up to 2304 sites, we show that the massive fermion phase spontaneously breaks this Ising symmetry, picking either antiferromagnetism or superconductivity, and that the transition at which both orders are simultaneously quantum critical belongs to a new "chiral spin-charge symmetric" universality class. We explain our observations using effective potential and renormalization group calculations within the framework of a continuum field theory.

DOI: 10.1103/PhysRevLett.128.117202

The study of graphene has triggered an avalanche of interest in the physics of massless relativistic fermions in two spatial dimensions, highlighting the connections between condensed matter and high energy physics theory, and the unity of physics across disparate energy scales [1–5]. While the simplest models of graphene result in massless Dirac fermions, a basic question that has been scrutinized heavily is how and when these low energy excitations can develop a mass gap [6–8]. Of particular interest in this Letter is the situation when strong electron-electron interaction drives the mass generation. The most common mechanism is through spontaneous symmetry breaking in which the order parameter couples to a mass term in the Dirac equation. Examples include the formation of Néel order [9,10] or a valence bond solid [11,12]. Typically the critical point between the massless Dirac phase and the symmetry broken state is described by some Gross-Neveu-Yukawa (GNY) field theory [13] (see, however, [14–16]).

The simplest route to the two-dimensional massless Dirac equation on a lattice is through the hopping of electrons,

$$H_0 = -\sum_{\langle i,j\rangle\alpha} t_{ij}(c^\dagger_{i\alpha}c_{j\alpha} + c^\dagger_{j\alpha}c_{i\alpha}), \tag{1}$$

with an appropriately chosen t_{ij}, where $c_{i\alpha}$ destroys an electron on lattice site i with spin $\alpha = \uparrow, \downarrow$. In this Letter we study the hopping matrix elements t_{ij} with a two-dimensional bipartite structure that preserves particle-hole symmetry and is independent of the electron spins. At low energies the electronic structure of such a model is described by spin degenerate ($N_f = 2$) four-component massless Dirac fermions. The most celebrated example of such a model is nearest-neighbor hopping on a honeycomb lattice with $t_{ij} = t$, which is a basic model for the electronic structure of graphene [1]. Another popular example is a square lattice with nearest-neighbor hoppings $t_{ij} = t\eta_{ij}$, where the phases η_{ij} realize a π flux on each fundamental plaquette [17]. To obtain a π flux on a square lattice, we can choose $\eta_{i,i+e_x} = 1$ and $\eta_{i,i+e_y} = (-1)^{i_x}$, where e_x and e_y are the unit vectors in the x and y direction, and i_x is the x component of i.

In addition to the usual lattice symmetries and time reversal, H_0 possesses certain internal symmetries that will play a central role in our work. Most well known is the $\mathrm{SU}(2)_s$ spin rotational symmetry, which is generated by $\vec{\mathcal{S}}_i = \frac{1}{2}c^\dagger_{i\alpha}\vec{\sigma}_{\alpha\beta}c_{i\beta}$. The model also has what is by now a well-known "hidden" $\mathrm{SU}(2)_c$ charge symmetry [18], which is generated by $\vec{\mathcal{C}}_i = \frac{1}{2}[\zeta_i(c^\dagger_{i\uparrow}c^\dagger_{i\downarrow} + c_{i\downarrow}c_{i\uparrow}), -i\zeta_i(c^\dagger_{i\uparrow}c^\dagger_{i\downarrow} - c_{i\downarrow}c_{i\uparrow}), c^\dagger_{i\uparrow}c_{i\uparrow} + c^\dagger_{i\downarrow}c_{i\downarrow} - 1]$, with $\zeta_i = \pm 1$ depending on the A and B sublattices and $i = \sqrt{-1}$. Finally, H_0 has an additional $\mathbb{Z}_2^{sc}$ spin-charge flip symmetry under which $c_{i\downarrow} \mapsto \zeta_i c^\dagger_{i\downarrow}$, $c_{i\uparrow} \mapsto c^\dagger_{i\uparrow}$, and the generators of spin and charge rotations are interchanged, $\vec{\mathcal{S}}_i \leftrightarrow \vec{\mathcal{C}}_i$. The $\mathrm{SU}(2)_s \times \mathrm{SU}(2)_c \times \mathbb{Z}_2^{sc}$ symmetries can be combined into an O(4) symmetry (see Supplemental Material [19]). This O(4) symmetry is most manifest when the hopping Hamiltonian is rewritten in terms of real "Majorana" modes γ^a_i, with $a = 1, 2, 3, 4$, and γ^a_i transforming in the vector representation of O(4), the hopping taking the form $H_0 = \sum_{\langle i,j\rangle a}(i/2)t_{ij}\gamma^a_i\gamma^a_j$.

Most often electron-electron interactions are added to Eq. (1) by the Hubbard-U term, $H_U = U\sum_i(n_{i\uparrow} - \frac{1}{2})(n_{i\downarrow} - \frac{1}{2})$. This term preserves the $\mathrm{SU}(2)_s$ and $\mathrm{SU}(2)_c$ symmetries, but being odd under the $\mathbb{Z}_2^{sc}$ acts like an Ising magnetic field that breaks the spin-charge flip symmetry. It is well known that repulsive-U interactions favor an antiferromagnetic "spin" order parameter $\vec{\phi}^s$, and attractive U favors a combined charge-density wave (CDW)–superconducting "charge" order parameter $\vec{\phi}^c$. We can understand how these orders couple to the fermions in a simple mean-field model, $H_{\rm MF} = H_0 + \sum_i \zeta_i(\vec{\phi}_i^s \cdot \vec{\mathcal{S}}_i + \vec{\phi}_i^c \cdot \vec{\mathcal{C}}_i)$. For $U > 0$, $\vec{\phi}^s \neq 0$ but $\vec{\phi}^c = 0$ (and vice versa for $U < 0$). Since H_0 realizes a $2+1$-dimensional Dirac dispersion, long range order sets in at a finite-$|U|$ phase transition which is described by the so-called "chiral-Heisenberg" GNY fixed point that has been the subject of intense numerical [20–23] and field theoretic studies [24–27]. In this Letter we look into the nature of the quantum critical phenomena when we add electron-electron interactions to Eq. (1) that preserve the full O(4) symmetry of the hopping problem, including the crucial $\mathbb{Z}_2^{sc}$ symmetry, which is absent in the usual Hubbard formulation.

Clearly the full O(4) symmetry of Eq. (1) will be preserved if we add interactions that depend only on $\sum_\alpha (c_{i\alpha}^\dagger c_{j\alpha} + c_{j\alpha}^\dagger c_{i\alpha})$ with i, j on opposite sublattices. To this end we focus on a sign-problem-free "designer Hamiltonian" (in natural units) which satisfies this criterion,

$$H_{\rm SC} = -\sum_{\langle i,j\rangle} \exp\left(\kappa\eta_{ij} \sum_{\alpha=\uparrow,\downarrow} (c_{i\alpha}^\dagger c_{j\alpha} + c_{j\alpha}^\dagger c_{i\alpha})\right). \quad (2)$$

Our model may be viewed as an interacting Hubbard-like model (identical Hilbert space) but with spin-charge flip symmetry present. Note that our model can be written as a sum of terms defined on bonds of the lattice that consist of fermion bilinears and four-, six- and eight-fermion interactions (but no higher order terms) [19]. For $\kappa \ll 1$ the fermion bilinear terms reproduce Eq. (1) with $t_{ij} = \kappa\eta_{ij}$, and since fermion interactions are perturbatively irrelevant at the massless fixed point, the semimetal phase must emerge at $\kappa \ll 1$. For $\kappa \gg 1$, we show using numerical simulations that the Dirac fermions acquire a mass, but because of the spin-charge flip symmetry *both* $\vec{\phi}^s$ and $\vec{\phi}^c$ are degenerate and the system breaks the $\mathbb{Z}_2^{sc}$ symmetry by picking one of the two ground states. We present numerical evidence below that the phase transition between Dirac semimetal and spin-charge flip broken phase is continuous and in a new universality in which both order parameters are simultaneously quantum critical. We note that other models preserving the spin-charge flip symmetry include a four-fermion model [19,28] and various fermion-boson models [29,30], although they do not harbor the new critical point.

Our designer Hamiltonian Eq. (2) was chosen because we can adapt a fermion bag quantum Monte Carlo (QMC) algorithm to study it [31,32]. By renormalization group (RG) arguments, Eq. (2) spin-charge is expected to capture universal aspects of the new quantum critical point [33]. The fermion bag algorithm is applicable to all Hamiltonians that are made up of only local terms whose fermionic degrees of freedom are exponentiated bilinears. While this is a limited family of systems, the algorithm is very efficient within its scope of applicability [31]. We expand the partition function $Z = {\rm tr} e^{-H_{\rm SC}/T}$ as $Z = \sum_k \int [d\tau] \times (-1)^k {\rm Tr}[H_{\rm SC}(\tau_k) \cdots H_{\rm SC}(\tau_2) H_{\rm SC}(\tau_1)]$. Here the notation $\int [d\tau]$ denotes time-ordered integration for times $1/T \geq \tau_k \geq \cdots \geq \tau_2 \geq \tau_1 \geq 0$. The expansion can be derived from the continuous-time interaction representation where $H_0 = 0$ and $H_{\rm int} = H_{\rm SC}$ [34–39], and also resembles the stochastic series expansion [40,41]. The algorithm then involves exploring a configuration space made up of the terms in the expansion and makes use of locality to compute transition probabilities as small determinants [31,32]. With two spin species, it is immediately evident that there is no sign problem in the expansion, because every term in the sum is the square of a real number. However, we note that even in models of the form Eq. (2) but with an odd number of flavors there is still no sign problem [42–45]. We compute two correlation functions of order parameters,

$$C_S = 2\langle \mathcal{S}_{i_0}^z \mathcal{S}_{i_1}^z \rangle, \qquad C_U = \langle \mathcal{U}_{i_0}^z \mathcal{U}_{i_1}^z \rangle, \quad (3)$$

where C_S measures the Néel order through the antiferromagnetic spin order parameter $\mathcal{S}_i^z$ and C_U measures the breaking of the spin-charge symmetry through the order parameter $\mathcal{U}_i = (n_{i\uparrow} - \frac{1}{2})(n_{i\downarrow} - \frac{1}{2})$, which is a four-fermion operator that is odd under $\mathbb{Z}_2^{sc}$, but invariant under $SU(2)_s \times SU(2)_c$. In Eq. (3), $i_0 = (0,0)$ and $i_1 = (L/2, 0)$ and we assume $L/2$ is even. We work at a finite inverse temperature $1/T = L$ and for numerical convenience we henceforth work with the tuning parameter $\mathbf{g} = 2\tanh(\kappa/2)$ instead of κ (see Supplemental Material [19]).

We first investigate the nature of the massive phase in our lattice model $H_{\rm SC}$, using the QMC method described above. We work at a coupling $\mathbf{g} = 1.6$, which is deep in the massive phase. As shown in Fig. 1, we find a finite value of C_U in the thermodynamic limit, which indicates that the Ising symmetry $\mathbb{Z}_2^{sc}$ is spontaneously broken. Further we find that C_S also scales to a finite value in the thermodynamic limit, which implies Néel order. Together we interpret this to imply that the system has to spontaneously choose between the charge and the spin sector, breaking $\mathbb{Z}_2^{sc}$, and forming either a Néel state or a superconductor-CDW state which breaks the corresponding SU(2) symmetry. Next, using QMC we study the nature of the phase transition between the Dirac semimetal and the massive phase. Figure 2 shows the data for C_S as a function of system size L. For large values of L, there is clear evidence that C_S converges to a nonzero constant at the coupling $g = 1.6$ (massive phase), while it scales to zero at the coupling $g = 1.48$ (Dirac semimetal). A good fit to the power-law $C_s = 0.67/L^{2.25}$ for $12 \leq L \leq 48$ with a

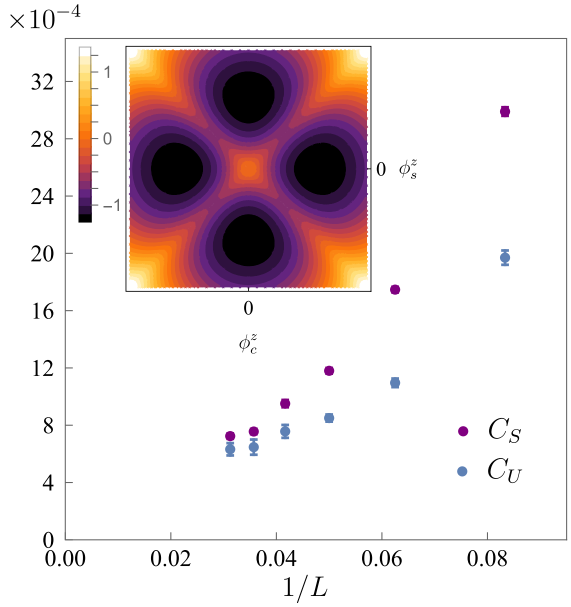

FIG. 1. Characterization of the massive phase from QMC and field theory. Finite size scaling data for C_S and C_U using the fermion bag QMC method for a coupling constant $\mathbf{g} = 1.6$. Both correlation functions scale to a finite value in the thermodynamic limit, indicating that the system breaks the $\mathbb{Z}_2^{sc}$ Ising symmetry as well as the SU(2) symmetry of spin and charge. Inset: effective potential for ϕ_s^z and ϕ_c^z, with $\vec{\phi}_{s,c} = (0, 0, \phi_{s,c}^z)$, when these order parameters are coupled to free massless Dirac fermions using the Yukawa coupling (4). Since the minimum of the potential is along the x and y axes, we conclude that the system condenses either $\vec{\phi}_s$ or $\vec{\phi}_c$ but not both, consistent with our interpretation of the QMC correlation functions.

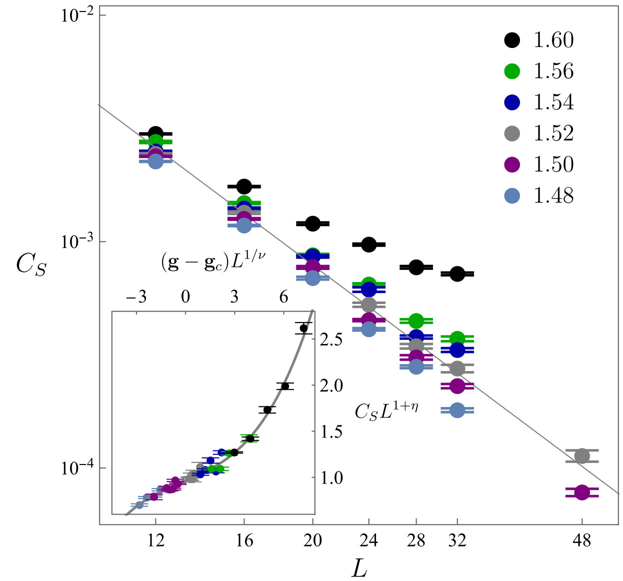

FIG. 2. C_S as a function of L on a log-log scale up to $L = 48$ for various values of $\mathbf{g}$. For large values of L we find that C_S decays to zero when $\mathbf{g} = 1.48$, while it saturates to a constant when $\mathbf{g} = 1.60$, with a phase transition around $\mathbf{g}_c \approx 1.52$ where the data fits to $C_S \approx 0.67/L^{2.25}$ (straight line in the plot). The inset shows that all of the data (after dropping $L = 12$) collapse to the universal scaling function discussed in the text with $\eta = 1.38(6)$, $\nu = 0.78(7)$, and $\mathbf{g}_c = 1.514(8)$, providing compelling evidence for a quantum critical point.

$\chi^2 = 0.95$ is found at the coupling $\mathbf{g} = 1.52$ as expected at a quantum critical point. A multiparameter scaling fit of all our data except for $L = 12$, to the form $C_S = L^{-(1+\eta)} f[(g - g_c)L^{1/\nu}]$ with $f(x) = f_0 + f_1 x + f_2 x^2 + f_3 x^3$, yields $\eta = 1.38(6)$, $\nu = 0.78(7)$, $\mathbf{g}_c = 1.514(8)$, $f_0 = 0.96(15)$, $f_1 = 0.073(26)$, $f_2 = 0.0012(43)$, and $f_3 = 0.0026(32)$ with a $\chi^2 = 1.25$. Interestingly, the large value of η clearly establishes that this criticality is not captured by the chiral-Heisenberg theory. We note that $\eta > 1$ although uncommon has been observed at certain critical points previously [26,46,47]. In the inset of Fig. 2 we show the scaling collapse of these data using the functional form of the multiparameter fit, providing strong evidence for a continuous quantum critical point.

To capture this observed phenomena, we formulate a field theory in the Euclidean space-time Lagrangian picture [19] in terms of the continuum fields that are expected to appear as long distance fluctuations near the critical point. These are eight-component fermion fields $\bar{\psi}$, ψ which are acted upon by tensor products of 4×4 Dirac matrices γ^μ and a spin Pauli matrix $\vec{\sigma}$. In terms of these fields, the spin and charge order parameter densities are given by $\vec{M}_s = \bar{\psi}_\alpha \vec{\sigma}_{\alpha\beta} \psi_\beta$ and $\vec{M}_c = [\psi_\downarrow^T \gamma^0 \psi_\uparrow + \bar{\psi}_\uparrow \gamma^0 \bar{\psi}_\downarrow^T, i(\psi_\downarrow^T \gamma^0 \psi_\uparrow - \bar{\psi}_\uparrow \gamma^0 \bar{\psi}_\downarrow^T), \bar{\psi}_\uparrow \psi_\uparrow + \bar{\psi}_\downarrow \psi_\downarrow]$. Then we can write down the following Yukawa-like Lagrangian density:

$$\mathcal{L}_Y = -\bar{\psi}_\alpha \gamma^\mu \partial_\mu \psi_\alpha + g_s \vec{\phi}_s \cdot \vec{M}_s + g_c \vec{\phi}_c \cdot \vec{M}_c, \tag{4}$$

where the first term is the free Dirac theory and the second term describes the interactions of the fermionic fields with critical bosonic fields $\vec{\phi}_s$ and $\vec{\phi}_c$ that describe the fluctuations of the antiferromagnetic and CDW-superconducting order parameters. In addition to these terms involving the fermionic fields, we supplement our theory with the kinetic terms and self-interactions of the bosonic fields,

$$\mathcal{L}_B = \sum_{a=s,c} \left(\frac{1}{2} \partial_\mu \vec{\phi}_a \cdot \partial^\mu \vec{\phi}_a + \frac{1}{2} m_a^2 \vec{\phi}_a \cdot \vec{\phi}_a + \frac{1}{4!} \lambda_a (\vec{\phi}_a \cdot \vec{\phi}_a)^2 \right) + \frac{1}{12} \lambda_{sc} (\vec{\phi}_s \cdot \vec{\phi}_s)(\vec{\phi}_c \cdot \vec{\phi}_c). \tag{5}$$

The first line in the above equation is the usual O(3) ϕ^4 model for spin and charge sectors. The second line describes a quartic interaction between the spin and charge bosonic fields that is allowed by symmetry. Previous studies of multicomponent field theories with fermions have not considered the above model [48–52].

The Euclidean Lagrangian density $\mathcal{L}_Y + \mathcal{L}_B$ is expected to describe the critical phenomena in our model. This theory is symmetric under $\mathrm{SU}(2)_s$ and $\mathrm{SU}(2)_c$; to impose the $\mathbb{Z}_2^{sc}$ we need to require, in addition, $g_s = g_c$, $\lambda_s = \lambda_c$, and $m_s = m_c$. Then this continuum theory possesses the full O(4) symmetry of our lattice Hamiltonian, and a thorough analysis of all the Yukawa couplings that are allowed by this O(4) symmetry can be found in [53]. When $m_{s,c}$ are large, the bosons will be gapped and we expect a fixed point with massless Dirac particles, which we identify with the semimetal phase in our lattice model. As $m_{s,c}$ is lowered we expect the bosons to condense, resulting in a massive phase. Interestingly, in this phase the Dirac fermions mediate an interaction between the $\vec{\phi}_{s,c}$ order parameters. To obtain the effective potential, we assume the condensed bosonic fields are constant in space-time, then we use the O(3) symmetry to rotate $\vec{\phi}_{s,c}$ fields so they point in the z direction. In this basis, the $\uparrow$ electrons feel a mass $\phi^+ = \phi_s^z + \phi_c^z$ and $\downarrow$ electrons experience $\phi^- = \phi_c^z - \phi_s^z$. Integrating out the fermions creates an identical effective potential for $\phi^\pm$, which means in the massive phase $\phi^\pm$ condense to the same magnitude but differ at most by a sign (which is determined spontaneously). In the $\phi_{c,s}^z$ language this implies that, in the massive phase in the presence of $\mathbb{Z}_2^{sc}$, the system spontaneously chooses to condense one of $\vec{\phi}_{s,c}$ and leave the other uncondensed. This is a remarkable mechanism of repulsion between the $\vec{\phi}_s$ and $\vec{\phi}_c$ that is generated by the interaction with fermions. The result of an explicit calculation [19] of the effective potential from the fermion determinant is plotted in the inset of Fig. 1, confirming the nature of the massive phase. If $g_s \neq g_c$, the Ising symmetry would be broken, the minima would not be degenerate, and the system would then favor the spin (charge) sector as happens in the repulsive (attractive) Hubbard model.

Since all the nonlinear couplings λ_s, λ_c, λ_{sc}, g_s, and g_c become marginal in four dimensions, we can study the critical region of $\mathcal{L}_Y + \mathcal{L}_B$ using the perturbative RG in $4-\varepsilon$ dimensions. We have obtained identical one-loop flow equations using both dimensional regularization with minimal subtraction [54] and a soft cutoff method [55] for the massless theory [19],

$$\frac{dg_s^2}{d\log\ell} = \varepsilon g_s^2 - \frac{1}{8\pi^2}[(2N_f+1)g_s^4 + 9g_s^2 g_c^2],$$

$$\frac{d\lambda_s}{d\log\ell} = \varepsilon\lambda_s - \frac{1}{8\pi^2}\left(\frac{11}{6}\lambda_s^2 + \frac{1}{2}\lambda_{sc}^2 + 4N_f g_s^2\lambda_s - 24N_f g_s^4\right),$$

$$\frac{d\lambda_{sc}}{d\log\ell} = \varepsilon\lambda_{sc} - \frac{1}{8\pi^2}\left[\frac{5}{6}(\lambda_s+\lambda_c)\lambda_{sc} + \frac{2}{3}\lambda_{sc}^2 + 2N_f(g_s^2+g_c^2)\lambda_{sc} - 24N_f g_s^2 g_c^2\right]. \tag{6}$$

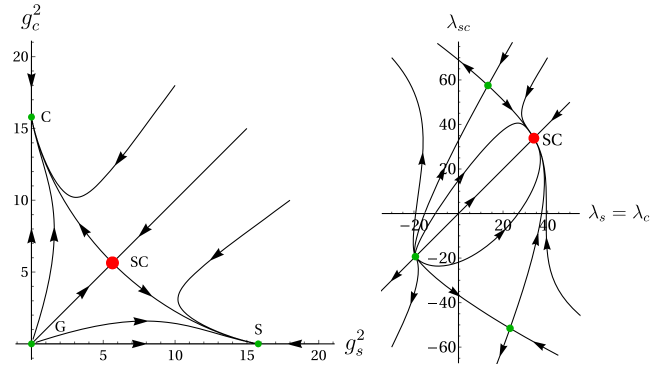

FIG. 3. Renormalization group flows of the couplings in the massless $\mathcal{L}_Y + \mathcal{L}_B$ theory close to four dimensions. Left: the one-loop flow of the Yukawa coupling g_s, g_c are independent of the λ and are shown. In addition to the unstable Gaussian fixed point (G) there are two chiral-Heisenberg fixed points corresponding to the transition from semimetal to Néel (S) and semimetal to CDW-superconductor (C). In addition there is a new fixed point (SC), which captures the chiral spin-charge symmetric universality, the focus of our study. In models with $\mathbb{Z}_2^{sc}$ symmetry like H_{SC} of Eq. (2), the flow is restricted to the diagonal $g_s^2 = g_c^2$ line, ensuring the stability of the SC fixed point and the inaccessibility of S and C in such spin-charge symmetric models. As expected, the SC fixed point is unstable to breaking of $\mathbb{Z}_2^{sc}$. Right: flow of the boson self interactions in the spin-charge symmetric sector with g_s and g_c fixed at their spin-charge symmetric fixed point values (SC). Together these graphs show that the SC fixed point is stable in the spin-charge symmetric sector and can hence be reached by tuning just one parameter, the mass of the boson. Being the only such fixed point, this qualifies SC as the universal theory of the quantum critical point found in our numerical work.

The flow equations for g_c^2 and λ_c can be obtained by exchanging the s and c subscripts using spin-charge flip symmetry. We now study the fixed points of these flow equations. We note that we can choose N_f in different ways: in $2+1$ dimensions, our case of interest, $N_f = 2$; on the other hand, our lattice model when extended to $3+1$ dimensions would give $N_f = 4$. An ε expansion with either choice can be formulated and does not affect our main conclusions, except for quantitative estimates for the critical exponents. We proceed with $N_f = 2$. Since the $g_{s,c}$ equation does not involve the quartic boson interactions, we can solve them separately. The Yukawa flow equations have four zeros in (g_s, g_c): (0,0) is the unstable Gaussian fixed point G, $(\frac{4}{7}\pi^2\varepsilon, \frac{4}{7}\pi^2\varepsilon)$ is a spin-charge symmetric fixed point (SC), and $(0, \frac{8}{5}\pi^2\varepsilon)$ (S) and $(\frac{8}{5}\pi^2\varepsilon, 0)$ (C) are chiral-Heisenberg fixed points, as shown in Fig. 3. We now ask whether there is a stable spin-charge symmetric fixed point in the bosonic sector when $g_{s,c}$ are evaluated at the SC values. Indeed, with this evaluation, there are four bosonic fixed points as shown in Fig. 3, but only one is stable, providing us with a unique fixed point that captures the universal aspects of the quantum critical point in our lattice model.

By studying the renormalization of the field strength and boson mass, we can compute the critical exponents η and ν. The critical exponents at leading order in ε are [19], $\eta = \frac{2}{7}\epsilon$, $\eta_\psi = \frac{3}{14}\epsilon$, $\frac{1}{\nu} = 2 - \frac{6}{7}\epsilon$. We note that the quantitative agreement for these exponents between the one-loop ε expansion and the numerical data is not great. But such discrepancy has been seen in other GNY type theories and can be attributed in part to the large value of η.

R. K. K. acknowledges NSF DMR-2026947, the Aspen Center for Physics (NSF Grant No. PHY-1607611) and G. Murthy for discussions. S. C. and H. L. are supported by the U.S. Department of Energy, Office of Science, Nuclear Physics program under Award No. DE-FG02-05ER41368. Research of E. H. at the Perimeter Institute is supported in part by the Government of Canada through the Department of Innovation, Science and Economic Development and by the Province of Ontario through the Ministry of Colleges and Universities. The authors thank F. Assaad, I. Herbut, L. Janssen, and M. Scherer for comments on the Letter. This work used computational resources provided by the Extreme Science and Engineering Discovery Environment (XSEDE) [56], which is supported by National Science Foundation Grant No. ACI-1548562.

[1] A. H. Castro Neto, F. Guinea, N. M. R. Peres, K. S. Novoselov, and A. K. Geim, The electronic properties of graphene, Rev. Mod. Phys. **81**, 109 (2009).

[2] N. P. Armitage, E. J. Mele, and A. Vishwanath, Weyl and Dirac semimetals in three dimensional solids, Rev. Mod. Phys. **90**, 015001 (2018).

[3] J. E. Drut and T. A. Lähde, Is Graphene in Vacuum an Insulator?, Phys. Rev. Lett. **102**, 026802 (2009).

[4] D. T. Son, Quantum critical point in graphene approached in the limit of infinitely strong Coulomb interaction, Phys. Rev. B **75**, 235423 (2007).

[5] W. Armour, S. Hands, and C. Strouthos, Monte Carlo simulation of the semimetal-insulator phase transition in monolayer graphene, Phys. Rev. B **81**, 125105 (2010).

[6] F. D. M. Haldane, Model for a Quantum Hall Effect without Landau Levels: Condensed-Matter Realization of the "Parity Anomaly", Phys. Rev. Lett. **61**, 2015 (1988).

[7] C. L. Kane and E. J. Mele, Quantum Spin Hall Effect in Graphene, Phys. Rev. Lett. **95**, 226801 (2005).

[8] S. Ryu, C. Mudry, C.-Y. Hou, and C. Chamon, Masses in graphenelike two-dimensional electronic systems: Topological defects in order parameters and their fractional exchange statistics, Phys. Rev. B **80**, 205319 (2009).

[9] S. Sorella and E. Tosatti, Semi-metal-insulator transition of the Hubbard model in the honeycomb lattice, Europhys. Lett. **19**, 699 (1992).

[10] Z. Y. Meng, T. C. Lang, S. Wessel, F. F. Assaad, and A. Muramatsu, Quantum spin liquid emerging in two-dimensional correlated Dirac fermions, Nature (London) **464**, 847 (2010).

[11] Z.-X. Li, Y.-F. Jiang, S.-K. Jian, and H. Yao, Fermion-induced quantum critical points, Nat. Commun. **8**, 314 (2017).

[12] T. Sato, M. Hohenadler, and F. F. Assaad, Dirac Fermions with Competing Orders: Non-Landau Transition with Emergent Symmetry, Phys. Rev. Lett. **119**, 197203 (2017).

[13] I. F. Herbut, Interactions and Phase Transitions on Graphene's Honeycomb Lattice, Phys. Rev. Lett. **97**, 146401 (2006).

[14] V. Ayyar and S. Chandrasekharan, Massive fermions without fermion bilinear condensates, Phys. Rev. D **91**, 065035 (2015).

[15] S. Catterall, Fermion mass without symmetry breaking, J. High Energy Phys. 01 (2016) 121.

[16] K. Slagle, Y.-Z. You, and C. Xu, Exotic quantum phase transitions of strongly interacting topological insulators, Phys. Rev. B **91**, 115121 (2015).

[17] J. B. Kogut and L. Susskind, Hamiltonian formulation of Wilson's lattice gauge theories, Phys. Rev. D **11**, 395 (1975).

[18] C. Yang and S. Zhang, SO(4) Symmetry in a Hubbard model, Mod. Phys. Lett. B **04**, 759 (1990).

[19] See Supplemental Material at http://link.aps.org/supplemental/10.1103/PhysRevLett.128.117202 for details about the connection of our model to the more conventional lattice Hamiltonian and continuum field theory, calculations of the effective potential and ϵ-expansion, and a table containing the QMC data.

[20] S. Sorella, Y. Otsuka, and S. Yunoki, Absence of a spin liquid phase in the Hubbard model on the honeycomb lattice, Sci. Rep. **2**, 992 (2012).

[21] F. F. Assaad and I. F. Herbut, Pinning the Order: The Nature of Quantum Criticality in the Hubbard Model on Honeycomb Lattice, Phys. Rev. X **3**, 031010 (2013).

[22] Y. Otsuka, S. Yunoki, and S. Sorella, Universal Quantum Criticality in the Metal-Insulator Transition of Two-Dimensional Interacting Dirac Electrons, Phys. Rev. X **6**, 011029 (2016).

[23] Y. Otsuka, K. Seki, S. Sorella, and S. Yunoki, Dirac electrons in the square-lattice Hubbard model with a d-wave pairing field: The chiral Heisenberg universality class revisited, Phys. Rev. B **102**, 235105 (2020).

[24] J. A. Gracey, Calculation of exponent eta to O(1/N**2) in the O(N) Gross-Neveu model, Int. J. Mod. Phys. A **06**, 395 (1991); **06**, 2755(E) (1991).

[25] B. Rosenstein, H.-L. Yu, and A. Kovner, Critical exponents of new universality classes, Phys. Lett. B **314**, 381 (1993).

[26] L. Janssen and I. F. Herbut, Antiferromagnetic critical point on graphene's honeycomb lattice: A functional renormalization group approach, Phys. Rev. B **89**, 205403 (2014).

[27] N. Zerf, L. N. Mihaila, P. Marquard, I. F. Herbut, and M. M. Scherer, Four-loop critical exponents for the Gross-Neveu-Yukawa models, Phys. Rev. D **96**, 096010 (2017).

[28] Z.-X. Li, S.-K. Jian, and H. Yao, Deconfined quantum criticality and emergent SO(5) symmetry in fermionic systems, arXiv:1904.10975.

[29] F. F. Assaad and T. Grover, Simple Fermionic Model of Deconfined Phases and Phase Transitions, Phys. Rev. X **6**, 041049 (2016).

[30] A. Goetz, S. Beyl, M. Hohenadler, and F. F. Assaad, Langevin dynamics simulations of the two-dimensional Su-Schrieffer-Heeger model, arXiv:2102.08899.

[31] E. Huffman and S. Chandrasekharan, Fermion bag approach to hamiltonian lattice field theories in continuous time, Phys. Rev. D **96**, 114502 (2017).

[32] E. Huffman and S. Chandrasekharan, Fermion-bag inspired Hamiltonian lattice field theory for fermionic quantum criticality, Phys. Rev. D **101**, 074501 (2020).

[33] R. K. Kaul, R. G. Melko, and A. W. Sandvik, Bridging lattice-scale physics and continuum field theory with quantum Monte Carlo simulations, Annu. Rev. Condens. Matter Phys. **4**, 179 (2013).

[34] N. V. Prokof'ev and B. V. Svistunov, Polaron Problem by Diagrammatic Quantum Monte Carlo, Phys. Rev. Lett. **81**, 2514 (1998).

[35] A. N. Rubtsov, V. V. Savkin, and A. I. Lichtenstein, Continuous-time quantum Monte Carlo method for fermions, Phys. Rev. B **72**, 035122 (2005).

[36] P. Werner, A. Comanac, L. de' Medici, M. Troyer, and A. J. Millis, Continuous-Time Solver for Quantum Impurity Models, Phys. Rev. Lett. **97**, 076405 (2006).

[37] M. Iazzi and M. Troyer, Efficient continuous-time quantum Monte Carlo algorithm for fermionic lattice models, Phys. Rev. B **91**, 241118(R) (2015).

[38] E. Burovski, E. Kozik, N. Prokofev, B. Svistunov, and M. Troyer, Critical Temperature Curve in BEC-BCS Crossover, Phys. Rev. Lett. **101**, 090402 (2008).

[39] O. Goulko and M. Wingate, Thermodynamics of balanced and slightly spin-imbalanced Fermi gases at unitarity, Phys. Rev. A **82**, 053621 (2010).

[40] A. W. Sandvik and J. Kurkijärvi, Quantum Monte Carlo simulation method for spin systems, Phys. Rev. B **43**, 5950 (1991).

[41] L. Wang, Y.-H. Liu, and M. Troyer, Stochastic series expansion simulation of the $t-v$ model, Phys. Rev. B **93**, 155117 (2016).

[42] E. F. Huffman and S. Chandrasekharan, Solution to sign problems in half-filled spin-polarized electronic systems, Phys. Rev. B **89**, 111101(R) (2014).

[43] Z.-X. Li, Y.-F. Jiang, and H. Yao, Solving the fermion sign problem in quantum Monte Carlo simulations by Majorana representation, Phys. Rev. B **91**, 241117(R) (2015).

[44] Z.-X. Li and H. Yao, Sign-problem-free fermionic quantum Monte Carlo: Developments and applications, Annu. Rev. Condens. Matter Phys. **10**, 337 (2019).

[45] Z.-C. Wei, Semigroup approach to the sign problem in quantum Monte Carlo simulations, arXiv:1712.09412.

[46] S. V. Isakov, R. G. Melko, and M. B. Hastings, Universal signatures of fractionalized quantum critical points, Science **335**, 193 (2012).

[47] I. Boettcher and I. F. Herbut, Superconducting quantum criticality in three-dimensional Luttinger semimetals, Phys. Rev. B **93**, 205138 (2016).

[48] B. Roy, Multicritical behavior of $\mathrm{z}2\times \mathrm{o}(2)$ Gross-Neveu-Yukawa theory in graphene, Phys. Rev. B **84**, 113404 (2011).

[49] B. Roy and V. Juričić, Strain-induced time-reversal odd superconductivity in graphene, Phys. Rev. B **90**, 041413(R) (2014).

[50] L. Classen, I. F. Herbut, L. Janssen, and M. M. Scherer, Mott multicriticality of Dirac electrons in graphene, Phys. Rev. B **92**, 035429 (2015).

[51] L. Janssen, I. F. Herbut, and M. M. Scherer, Compatible orders and fermion-induced emergent symmetry in Dirac systems, Phys. Rev. B **97**, 041117(R) (2018).

[52] B. Roy, P. Goswami, and V. Juričić, Itinerant quantum multicriticality of two-dimensional Dirac fermions, Phys. Rev. B **97**, 205117(R) (2018).

[53] H. Liu, A spin-charge flip symmetric fixed point in $2+1$d with massless Dirac fermions, in *38th International Symposium on Lattice Field Theory* (2021), arXiv:2111.02142, https://pos.sissa.it/396/.

[54] J. Zinn-Justin, *Quantum Field Theory and Critical Phenomena* (Clarendon Press, Oxford, 2002).

[55] M. Vojta, Y. Zhang, and S. Sachdev, Renormalization group analysis of quantum critical points in d-wave superconductors, Int. J. Mod. Phys. B **14**, 3719 (2000).

[56] J. Towns, T. Cockerill, M. Dahan, I. Foster, K. Gaither, A. Grimshaw, V. Hazlewood, S. Lathrop, D. Lifka, G. D. Peterson, R. Roskies, J. R. Scott, and N. Wilkins-Diehr, Xsede: Accelerating scientific discovery, Comput. Sci. Eng. **16**, 62 (2014).